Analysis of DWT-GLCM-Tamura and Angle Features for Variety Identification of Seeds

Archana Chaugule and S.N. Mali
Sinhgad Institute of Technology and Science, Narhe, Pune, 411041 Maharashtra, India

Abstract: This research proposes an algorithm to implement feature extraction technique using discrete wavelet-GLCM-Tamura and angle and use the extracted features to represent the image for classification of seeds. A total of 69 discrete wavelet-GLCM-Tamura and 12 angle features were extracted from the high-resolution images of paddy seeds. These features were employed along with ANN to identify paddy varieties. These researches is aimed at comparing discrete wavelet-GLCM-Tamura and angle features using ANN for discriminating Indian paddy varieties and also evaluate variety-wise classification of individual grains. The classification of four paddy (rice) grains, viz. Karjat-6 (K6) and Ratnagiri-2 (R2), Ratnagiri-4 (R4) and Ratnagiri-24 (R24) was done and the features were evaluated in terms of accuracy. From the entire feature models, most suitable feature was identified for accurate classification. Angle features gave the best classification using ANN among both the feature sets.

Key words: Angle, DWT, GLCM, neural network, Tamura

INTRODUCTION

The objective of this research was to identify and classify kernels of four paddy grain types using wavelet texture features and angle features. The goal was to minimize the losses incurred during farming by sowing proper type of seeds in the farm (Chaugule and Mali, 2014). Classification of agricultural materials was done with the help of wavelet textural features (Borah *et al.*, 2007; Cao *et al.*, 2012; Choudhary *et al.*, 2008, 2009; Zheng *et al.*, 2006). Wavelet analysis is a popular tool for categorization and classification of image texture (Mallat, 1989; Mojsilovic *et al.*, 2000). Using discrete wavelet transforms, image textures can be analyzed at multiple resolutions. Therefore, the wavelet features can be used for exploring their efficiency for classification of grains.

Wavelets can inspect data at various scales and frequencies (Sarlashkar *et al.*, 1998). Truncation of high frequency components from the wavelet transforms, filter out rotation and scaling variations in the images. This is due to low frequency components being spread in time domain and high frequency components being concentrated in the time domain. Therefore, high frequency components can be truncated.

Textural features (Majumdar and Jayas, 1999, 2000a) and even color features have been used (Majumdar and Jayas, 2000b) by some researchers for classification purposes. The main focus of previously published research was to use statistical pattern recognition technique to determine the potential of morphological features to classify different grain species, classes, varieties, spoiled grains and impurities. All these features have been integrated to a single classification vector for grain kernel identification (Paliwal *et al.*, 1999).

Statistical pattern classifiers which are based on Bayes' minimum error rule (Duda and Hart, 1973) have so far been the tool of choice for most of the research in this field. Some of the recent research (Jayas *et al.*, 2000; Paliwal *et al.*, 2001) however, has shown the potential of using ANN for classification of agricultural products. ANN has the potential to solve problems in which some inputs and the related values of output are known.

The color, size, shape and textural parameters of the agricultural products are not ruled by a unique mathematical function. This natural inconsistency in form is a challenge for any machine vision system to make out and categorize natural entities like cereal grains (Paliwal *et al.*, 2001). Most of the of research has gone into finding the potential of different features to classify different grain species, varieties and damaged grains using statistical pattern recognition techniques.

To a large degree, the success of any classification procedure depends on the classification criterion chosen for the task. A classification criterion classifies the objects into two or more classes, based on the features extracted from them.

ANN classifiers which are considered as an extension of many classification techniques are budding as the appropriate classifiers for pattern recognition.

Corresponding Author: Archana Chaugule, Sinhgad Institute of Technology and Science, Narhe, Pune, 411041 Maharashtra, India

It is important to explore the applicability of various NN architectures for classification of agricultural products including cereal grains, due to the increasing popularity of NN techniques in image analysis. Presently, the identification and grading of cereal grains is done manually in India. This task is subjective and time consuming. A machine vision system can be used instead of this labor-intensive evaluation of grain samples in the grain industry. As compared to most of their statistical counterpart, neural networks which perform faster classification, might offer a way out to the problem of slow classification (Paliwal *et al.*, 2001).

Hypothesis:
- Discrete Wavelet-GLCM-Tamura features can increase the accuracy of the classification
- Angle features can increase the accuracy of the classification as compared to Discrete Wavelet-GLCM-Tamura features

To prove this hypothesis, the decided objectives were to extract a total of 69 Discrete Wavelet-GLCM-Tamura features, extract a total of 12 angle features, evaluate the classification accuracy of both the feature sets and ANN and find the most suitable feature from the Discrete Wavelet-GLCM-Tamura and angle features for accurate classification.

MATERIALS AND METHODS

The proposed method includes two major algorithms for feature extraction which include Discrete Wavelet-GLCM-Tamura and angle. The block diagram of both the schemes is shown in Fig. 1 and 2, respectively.

Material and grain samples: The unclean commercial samples of four paddy grains, Karjat-6(K6), Karjat-2(K2), Ratnagiri-4(R4) and Ratnagiri-24(R24) used in this study were provided by the Seed Testing Laboratory-pune, India. The images were obtained using a Sony Make 18.9 Megapixels Digital camera. The camera was positioned horizontal to the plane. The light source was not defined as such the images were taken from variable illumination.

Image pre-processing: Image segmentation was done with the help of thresholding, before extracting the object features and any necessary morphological filtering was also done in the pre-processing phase. A total of 69 Discrete Wavelet-GLCM-Tamura and 12 Angle features were extracted and then used for assessing the performance.

Wavelet analysis: Wavelet analysis is a signal analysis tool for characterization of image texture at multiple resolutions. The Continuous Wavelet Transforms (CWT) of a signal x (n) is as follows:
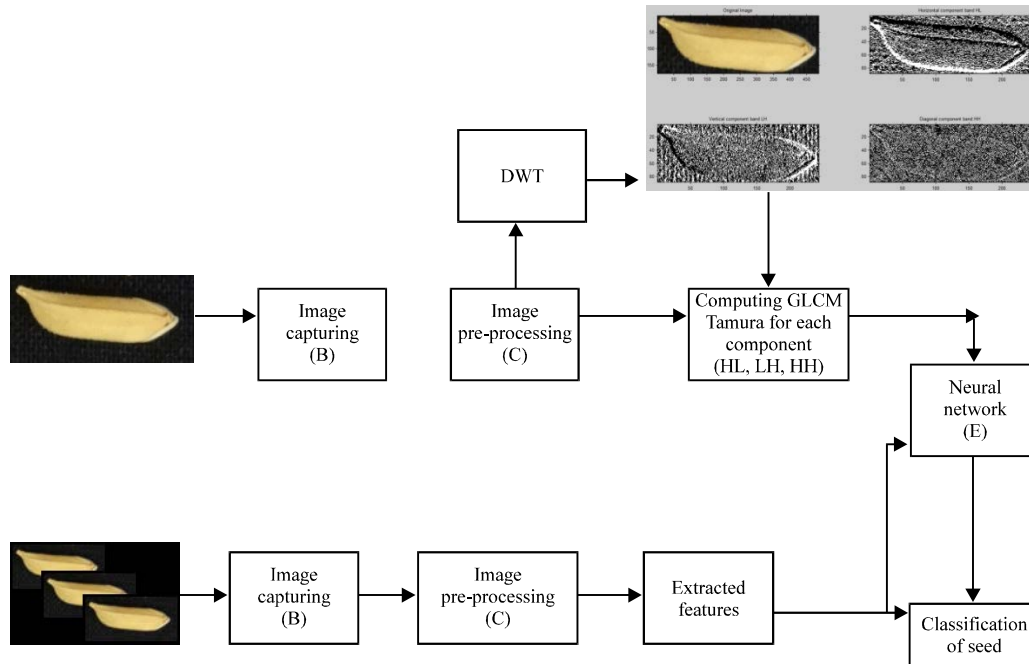

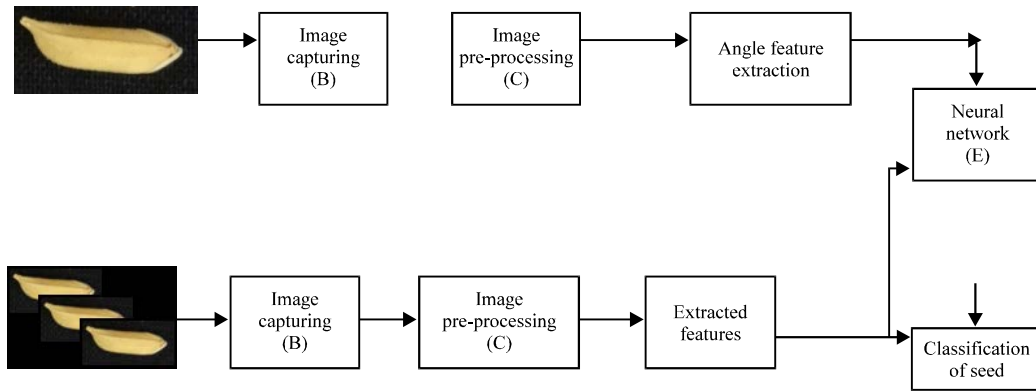Fig. 1: Block diagram for classification using Discrete Wavelet-GLCM-tamura features

Fig. 2: Block diagram for classification using angle features

$$W(s,t) = \frac{1}{\sqrt{s}} \int_{-\infty}^{\infty} x(n) \psi_{t,s}(n) dn \qquad (1)$$

Where:
x(n)   = The time signal
W(s, t) = The CWT coefficients of that signal
t   = The translation parameter
s   = The scale parameter

$$\psi_{s,t}(n) dn = \psi\left(\frac{n-1}{s}\right) \qquad (2)$$

Where:
ψ   = The mother wavelet translated by t and scaled by s
W(t, s) = The cross-correlation between the signal and the mother wavelet translated by 't' and scaled by 's' (Gonzalez *et al.*, 2004)

Although, the CWT can be implemented in discrete format, there is too much redundant information in the decomposed signals. As a result, the DWT is used with down-sampling at each level of decomposition to remove the redundant information (Walker, 1999). Discrete Wavelet Transforms (DWT) of images are implemented using digital filters and downsamplers.

The one-dimensional DWT provides two sets of coefficients at each level of decomposition, namely:

- Approximation (A)
- Horizontal (H)
- Vertical (V)
- Diagonal (D) (Gonzalez *et al.*, 2004)

The images of each kernel were subjected to single-level discrete 2-D wavelet decomposition with respect to first-order daubechies wavelet (db1). The approximation coefficients, details coefficients matrices (horizontal, vertical and diagonal) were obtained by wavelet decomposition at level 4. Twenty GLCM and three Tamura features were computed for each (horizontal, vertical and diagonal) bands.

Texture features extraction: Texture features included twenty GLCM and three Tamura features. GLCM features are as listed below, the details of which are as described in by Chaugule and Mali (2014).

Gray Level Concurrence Matrix (GLCM): They are contrast, correlation, energy, homogeneity, entropy for four offsets {(0°); (45°); (90°); (135°)} and are listed in Table 1. Similarly GLCM features with their expressions:

$$\sum_{n=0}^{G-1} n^2 \left\{ \sum_{i=1}^{G} \sum_{j=1}^{G} P(i,j) \right\}, |i-j| = n \qquad (3)$$

Correlation:

$$\sum_{i=0}^{G-1} \sum_{j=0}^{G-1} \frac{(i-\mu_i)(j-\mu_j)P(i,j)}{\sigma_i \sigma_j} \qquad (4)$$

Energy:

$$\sum_{i=0}^{G-1} \sum_{j=0}^{G-1} \{P(i,j)\}^2 \qquad (5)$$

Homogeneity:

$$\sum_{i}^{G-1} \sum_{j}^{G-1} \frac{P(i,j)}{1+|i-j|} \qquad (6)$$

Entropy:

$$-\sum_{i=0}^{G-1} \sum_{j=0}^{G-1} P(i,j) \times \log(P(i,j)) \qquad (7)$$

Similarly for vertical band contrast, correlation, energy, homogeneity, entropy for four offsets {(0°); (45°); (90°); (135°)} are symbolized from contrast 5-8, correlation 5-8, energy 5-8, homogeneity 5-8, entropy 5-8,

Table 1: The GLCM features with their symbols for horizontal band

Symbol	Feature
Contrast 1	Contrast for offset (0°) for horizontal band
Correlation 1	Correlation for offset (0°) for horizontal band
Energy 1	Energy for offset (0°) for horizontal band
Homogeneity 1	Homogeneity for offset (0°) for horizontal band
Entropy 1	Entropy for offset (0°) for horizontal band
Contrast 2	Contrast for offset (45°) for horizontal band
Correlation 2	Correlation for offset (45°) for horizontal band
Energy 2	Energy for offset (45°) for horizontal band
Homogeneity 2	Homogeneity for offset (45°) for horizontal band
Entropy 2	Entropy for offset (45°) for horizontal band
Contrast 3	Contrast for offset (90°) for horizontal band
Correlation 3	Correlation for offset (90°) for horizontal band
Energy 3	Energy for offset (90°) for horizontal band
Homogeneity 3	Homogeneity for offset (90°) for horizontal band
Entropy 3	Entropy for offset (90°) for horizontal band
Contrast 4	Contrast for offset (135°) for horizontal band
Correlation 4	Correlation for offset (135°) for horizontal band
Energy 4	Energy for offset (135°) for horizontal band
Homogeneity 4	Homogeneity for offset (135°) for horizontal band
Entropy 4	Entropy for offset (135°) for horizontal band

respectively. And for diagonal band are symbolized from contrast 9-12, correlation 9-12, energy 9-12, homogeneity 9-12 and entropy-12.

Tamura: The set of perceptual texture features that were used for the present study are coarseness, contrast and directionality and are taken from.

Coarseness: It is distance of spatial variations of grey levels which measures the texture scale. The procedure to evaluate the coarseness is as follows: At each pixel (x, y), six averages for the windows of size $2^n \times 2^n$, $n = 0, 1, ..., 5$, around the pixel are computed. The average is given as:

$$A(x,y) = \sum_{i1=x-2^{n-1}}^{x+2^{n-1}-1} \sum_{j1=y-2^{n-1}}^{y+2^{n-1}-1} \frac{f1(i1,j1)}{2^{2n}} \tag{8}$$

where $f1(i1, j1)$ is gray level value at pixel (x, y). Absolute differences $E_n(x, y)$ between the pairs of non overlapping averages in the horizontal and vertical directions are computed for each pixel which is given as follows:

$$E_{n,h}(x,y) = \left| A_n\left(x+2^{n-1},y\right) - A_n\left(x-2^{n-1},y\right) \right| \tag{9}$$

$$E_{n,v}(x,y) = \left| A_n\left(x,y+2^{n-1}\right) - A_n\left(x,y-2^{n-1}\right) \right| \tag{10}$$

At each pixel, the value of n that maximises the difference $E_n(x, y)$ in either direction is found and the best size is set as 2^n:

$$Sl_{best}(x,y) = 2^n \tag{11}$$

The coarseness feature is computed by averaging $Sl_{best}(x, y)$ over the entire image:

$$Coarseness = \frac{1}{m \times n} \sum_{i1=1}^{m} \sum_{j1=1}^{n} Sl_{best}(i1,j1) \tag{12}$$

Contrast: Contrast measures how grey levels g; $g = 0, 1, ..., g_{max}$, vary in the image and to what amount their variation is influenced to black or white. The variance, σ^2 and kurtosis, μ_4/σ_4 are used to define the contrast. The value $n1 = 0.25$ is suggested as the best for discriminating the textures:

$$Contrast = \frac{\sigma}{\left(\dfrac{\mu_4}{\sigma_4}\right)^{n1}} \tag{13}$$

Where:
σ = The standard deviation
μ_4 = The fourth moment about the mean
σ_4 = The variance squared

Directionality: Directionality is invariant to orientation (Tamura *et al.*, 1978). Firstly, each sub-image was convolved with an edge filter to calculate the horizontal and vertical differences, d_h and d_v. The convolution of the image $X(n_0, n_1)$ is done with the following 3×3 operators:

$$\begin{array}{cccccc} -1 & 0 & 1 & 1 & 1 & 1 \\ -1 & 0 & 1 & 0 & 0 & 0 \\ -1 & 0 & 1 & -1 & -1 & -1 \end{array}$$

And then for every position (n_0, n_1):

$$\theta = \frac{\pi}{2} + \tan^{-1} \frac{d_v(n_0,n_1)}{d_h(n_0,n_1)} \tag{14}$$

is calculated. These values are then histogrammized in a sixteen bin histogram and then, the directionality is calculated as the sum of second moments around each peak from valley to valley.

Feature extraction using DWT-GLCM and TAMURA: In the decomposition of discrete wavelet, the output is the coefficients (approximation, horizontal, vertical and diagonal) of the original image. The approximation carries little energy so is skipped from the analysis. The GLCM descriptors like contrast, correlation, energy, homogeneity and entropy for four offsets as shown in Table 1 are calculated for horizontal, vertical and diagonal coefficient. The expressions for GLCM features are shown in Eq. 3-7.
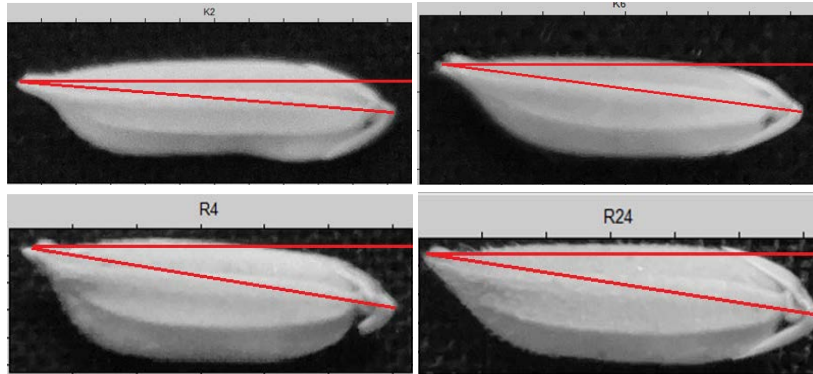
Fig. 3: Horizontal-vertical angle

Similarly tamura features like coarseness, contrast and directionality are calculated for horizontal, vertical and diagonal coefficient thus giving total 69 features which are listed as. DWT-GLCM-TAMURA = {contrast 1, correlation 1, energy 1, homogeneity 1, entropy 1, contrast 2, correlation 2, energy 2, homogeneity 2, entropy 2, contrast 3, correlation 3, energy 3, homogeneity 3, entropy 3, contrast 4, correlation 4, energy 4, homogeneity 4, entropy 4, contrast 5, correlation 5, energy 5, homogeneity 5, entropy 5, contrast 6, correlation 6, energy 6, homogeneity 6, entropy 6, contrast 7, correlation 7, energy 7, homogeneity 7, entropy 7, contrast 8, correlation 8, energy 8, homogeneity 8, entropy 8, contrast 9, correlation 9, energy 9, homogeneity 9, entropy 9, contrast 10, correlation 10, energy 10, homogeneity 10, entropy 10, contrast 11, correlation 11, energy 11, homogeneity 11, entropy 11, contrast 12, correlation 12, energy 12, homogeneity 12, entropy 12, coarseness 1, contrast 1, directionality 1, coarseness 2, contrast 2, directionality 2, coarseness 3, contrast 3, directionality 3}.

Feature extraction using angle features
Horizontal-vertical angle: Figure 3 shows the horizontal-vertical angle for a sample of all the four varieties. The following steps are used to extract this feature:

$$\theta = \text{Cos}^{-1}\left(A \times \frac{B}{|A|} \times |B|\right) \qquad (15)$$

Where:

$$A \times B = p1 \times p2 + q1 \times q2$$

$$|A| = \sqrt{(p1 \times p1) + (q1 \times q1)}$$

$$|B| = \sqrt{(p2 \times p2) + (q2 \times q2)}$$

θ is the angle between A and B. The calculated angle in radians is multiplied by 180/pi to convert to degrees:

$$(\theta) = \theta \frac{180}{pi} \qquad (16)$$

Similarly, the distance between two lines is calculated by taking the difference of the 'y' coordinates of the two lines. The 'y' coordinates used are calculated previously by Bresenham's algorithm. Then, the mean mode and median of the difference are calculated.

Mean (μ): Mean is the average vertical difference value:

$$\mu = \sum_{i=1}^{m} \frac{d_i}{m} \qquad (17)$$

Where, d_i is the vertical difference between two vectors at ith horizontal coordinates.

Mode: Mode is the most frequent vertical difference value:

$$\text{Mode} = L + \frac{f1 - f0}{2 \times f1 - f0 - f2} \times i \qquad (18)$$

Where
L = Lower limit of the class
f1 = Frequency of the modal class
f0 = Frequency of the class preceding the modal class
f2 = Frequency of the class succeeding the modal class

Median: Median is the value of its middle term after sorting the vertical difference vector:

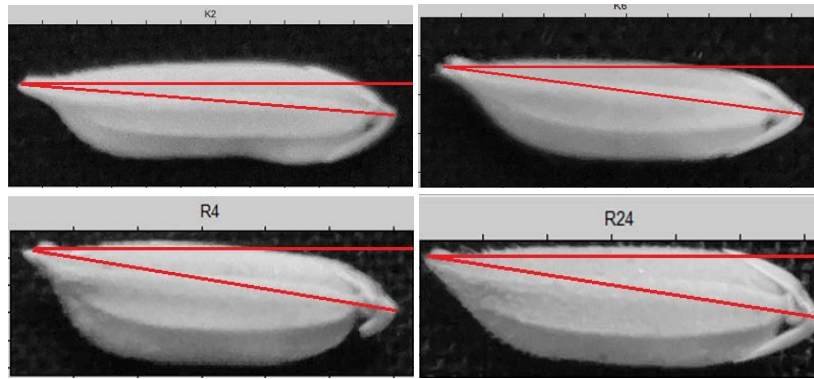$$\text{Median} = \left(\frac{i+1}{2}\right)^{\text{TH}} \text{term, if i is odd}$$

Or:

Fig. 4: Front-rear angle

$$\text{Median} = \frac{1}{2}\left[\begin{array}{c} \text{Value of} \left(\dfrac{i}{2}\right)^{\text{TH}} \text{Term} + \\[4pt] \text{value of} \left(\dfrac{i}{2}+1\right)^{\text{TH}} \text{term} \end{array} \right], \text{ if i is even} \quad (19)$$

Thus, the feature vector consists of angle and distance between two lines.

Front-rear angle: Figure 4 shows the calculated front and rear angles for a sample of all the four varieties. The angle calculation is shown in Eq. 16. Mean (μ) is the average angle value:

$$\mu = \sum_{i=1}^{m} \frac{\text{Angle}_i}{i} \quad (20)$$

where angle$_i$ is the ith angle in front and rear part.

Standard deviation (σ): Standard deviation is a measure of how spread-out numbers are:

$$\sigma = \sqrt{\text{var}} \quad (21)$$

Variance (var): Variance is the average of squared difference from mean:

$$\text{Var} = \frac{1}{m}\sum_{i=1}^{m}\left(\text{Angle}_i - \mu\right)^2 \quad (22)$$

The HOR-VER-FRONT-REAR-ANGLE = {angle, μ_y, mode$_y$, median$_y$, sum_rear, mean_rear, stddev_rear, var_rear, sum_front, mean_front, stddev_front, var_front}.

Neural network architectures: The architecture used was same as in previous literature (Chaugule and Mali, 2014).

Two-layer backpropagation supervised neural networks with a single hidden layer of twenty neurons were used to train the network. To provide a realistic estimate of the performance, the trained neural network was tested with the testing samples which had samples apart from the training samples. The data presented is from confusion matrix which was plotted across all samples to measure how well the neural network has fit the data. The configuration used was as follows.

Artificial neural network configuration: Number of hidden layer = 1, number of neurons = 20, error function = mean squared error, validation check stops, transfer function hyperbolic tangent sigmoid. To study the effect of various parameters, first discrete wavelet-GLCM-tamura and then, angle feature set were used for categorizing the grains. These feature sets are referred to as DWT-GLCM-tamura and angle. To evaluate the classification accuracy of discrete wavelet-GLCM-tamura and angle feature set and neural network, color images of K6, K2, R4 and R24 were taken. The input to the neural networks was the 69 discrete wavelet-GLCM-tamura and then, the 12 angle features that were extracted for each kernel. From each set 70% kernels were used for training and 30% kernels for testing of each grain. The 5 fold cross-validations were done to test the performance. Classification was done using a two-layer BPN with LM training functions and the results of the same were compared for different feature sets.

RESULTS AND DISCUSSION

Using the selected ANN configuration, the effect of proposed features on the recall and accuracy of class is studied. The assessment criteria are defined as follows:

Recall: The recall is how good a test is at detecting the positives. It relates to the test's ability to identify positive results:

Table 2: Recall of individual grains

Seeds	1	2	3	4	5
DWT-GLCM-tamura					
K6	51.9	59.3	74.1	55.6	59.3
K2	83.3	100.0	77.8	100.0	94.4
R24	100.0	90.0	100.0	100.0	100.0
R4	66.7	56.6	61.1	50.0	38.9
Angle					
K6	100.0	100.0	100.0	100.0	100.0
K2	72.2	83.3	88.9	94.4	77.8
R24	90.0	80.0	95.0	90.0	95.0
R4	88.9	83.3	94.4	94.4	94.4

Table 3: Comparison with other methods

Author	Seed	Feature	Method	Accuracy	No. of features
Cao *et al.* (2012)	Corn	Color	DWT and BPNN	94.5%	20
Auttawaitkul *et al.* (2014)	Rice	Color and Shape	--	91-97%	--
Liu *et al.* (2015)	Soyabean	Color, shape and texture	BPNN	97.25%	14
Huang (2012)	Areca nuts	Color and shape	ANN	90.9%	9
Wiwart *et al.* (2012)	Wheat	Color and shape analysis	Principal component	90.27% color and 98.98%, shape	20
Li *et al.* (2012)	Cotton	Color and shape	BPNN	90%	26
Szczypinski and Zaptoczny (2012)	Barley	Texture	Wrinkle detection	93%	--
Gunes *et al.* (2014)	Wheat	Texture	K-NN	80%	--
Khunkhett and Remsungnen (2014)	Rice	Color and shape	--	82-98%	7
Proposed method DWT-GLCM-tamura	Paddy	DWT-GLCM-tamura	BPNN	78.3%	69
Proposed method angle	Paddy	Angle	BPNN	95.2%	12

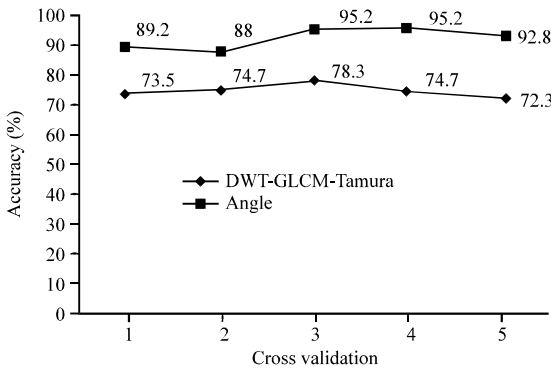
Fig. 5: Accuracy comparison plot

$$Recall = \frac{No.of\ true\ positive}{No.of\ true\ positive + No.of\ false\ negatives} \quad (23)$$

Accuracy: The accuracy is the number of correctly classified seeds upon the number of testing seeds:

$$Accuracy = \left(\begin{array}{c} No.of\ true\ positives\ + \\ No.of\ true\ negative \end{array} \right) / \left(\begin{array}{c} No.of\ true\ positives\ + \\ No.of\ true\ negative\ + \\ No.of\ false\ positives \end{array} \right) + n \quad (24)$$

The effects of various features on the accuracy of the variety-wise classification were studied using the selected ANN configuration described above. As mentioned earlier, five pairs of training/test data (5 fold cross-validations) were used for this study. Table 2 presents the representative results of testing of ANNs with features. Table 2 shows the recall of individual grains.

Figure 5 shows the accuracy comparison plot between DWT-GLCM-tamura features and angle features for 5 cross validations. The results showed that the accuracy of classification of the ANN was best most of the time when angle features were used in training and testing of the ANN and decreased for DWT-GLCM-tamura features. Table 3 shows comparison with the other methods. It can be seen that the proposed method-angle features has maximum accuracy as compared to others, except for the method in (Auttawaitkul *et al.*, 2014; Liu *et al.*, 2015) which had 97% accuracy for color, shape and texture but, it had number of features as fourteen. The number of features for the proposed method found is twelve while by the method proposed in (Huang, 2012) the number of features is nine, but the accuracy is 90.9% which is less than that of the proposed method. Thus a tradeoff between the accuracy and number of features is established by the proposed method.

CONCLUSION

In addition to the DWT-GLCM-tamura features, angle features were also extracted from images of individual

grains. The different feature sets were assessed for classification of grains. The presented method for the varietal identification of paddy shows around 78.3% accuracy for DWT-GLCM-Tamura features and 95.2% accuracy for Angle features. The most acceptable results were given by the measurement of angle features. DWT-GLCM-tamura feature set gave lower accuracy than other set. Thus, it can be concluded that angle features have a considerable role in classifying the paddy varieties than the DWT-GLCM-tamura features, calculated. Thus, angle features have the prospective to improve the accuracy of classification of the machine vision systems used for classification of four paddy grains. This also proves that instead of DWT (time-frequency domain), spatial domain is sufficient for classification of seeds.

ACKNOWLEDGEMENTS

REFERENCES

Auttawaitkul, Y., S. Buochareon, T. Maneechukate and N. Dussadee, 2014. Non-destructive identification of breeder rice seed using transparent image analysis. Proceedings of the 2014 4th Joint International Conference on Information and Communication Technology, Electronic and Electrical Engineering (JICTEE), March 5-8, 2014, IEEE, Sansai, Thailand, ISBN:978-1-4799-3855-1, pp: 1-4.

Borah, S., E.L. Hines and M. Bhuyan, 2007. Wavelet transform based image texture analysis for size estimation applied to the sorting of tea granules. J. Food Eng., 79: 629-639.

Cao, W., C. Zhang, J. Wang, S. Liu and X. Xu, 2012. Purity identification of maize seed based on discrete wavelet transform and BP neural network. Trans. Chinese Soc. Agric. Eng., 28: 253-258.

Chaugule, A. and S.N. Mali, 2014. Evaluation of texture and shape features for classification of four paddy varieties. J. Eng., 2014: 1-9.

Choudhary, R., J. Paliwal and D.S. Jayas, 2008. Classification of cereal grains using wavelet, morphological, colour and textural features of non-touching kernel images. Biosyst. Eng., 99: 330-337.

Choudhary, R., S. Mahesh, J. Paliwal and D.S. Jayas, 2009. Identification of wheat classes using wavelet features from near infrared hyperspectral images of bulk samples. Biosyst. Eng., 102: 115-127.

Duda, R.O. and P.E. Hart, 1973. Pattern Classification and Scene Analysis. 2nd Edn., John Wiley and Sons, New York, ISBN: 0-471-22361-1, pp: 482.

Gonzalez, R.C., R.E. Woods and S.L. Eddins, 2004. Digital Image Processing Using MATLAB. Pearson Prentice Hall, New Jersey, USA., ISBN-13: 978-0130085191, Pages: 609.

Gunes, E.O., S. Aygun, M. Kirci, A. Kalateh and Y. Cakir, 2014. Determination of the varieties and characteristics of wheat seeds grown in Turkey using image processing techniques. Proceedings of the Third International Conference on Agro-Geo informatics, August 11-14, 2014, IEEE, Istanbul, Turkey, ISBN:978-1-4799-4157-5, pp: 1-4.

Huang, K.Y., 2012. Detection and classification of areca nuts with machine vision. Comput. Math. Appl., 64: 739-746.

Jayas, D.S., J. Paliwal and N.S. Visen, 2000. Multi-layer neural networks for image analysis of agricultural products. J. Agric. Eng. Res., 77: 119-128.

Khunkhett, S. and T. Remsungnen, 2014. Non-destructive identification of pure breeding rice seed using digital image analysis. Proceedings of the 2014 4th Joint International Conference on Information and Communication Technology, Electronic and Electrical Engineering (JICTEE), March 5-8, 2014, IEEE, Khonkaen, Thailand, ISBN:978-1-4799-3855-1, pp: 1-4.

Li, J., B. Chen, L. Shao, X. Tian and Z. Kan, 2012. Variety identification of delinted cottonseeds based on BP neural network. Trans. Chin. Soc. Agric. Eng., 28: 265-269.

Liu, D., X. Ning, Z. Li, D. Yang and H. Li et al., 2015. Discriminating and elimination of damaged soybean seeds based on image characteristics. J. Stored Prod. Res., 60: 67-74.

Majumdar, S. and D.S. Jayas, 2000a. Classification of cereal grains using machine vision. I. Morphology models. Trans. Am. Soc. Agric. Eng., 43: 1669-1675.

Majumdar, S. and D.S. Jayas, 2000b. Classification of cereal grains using machine vision.II. Color models. Trans. Am. Soc. Agric. Eng., 43: 1677-1680.

Majumdar, S., D.S. Jayas and S.J. Symons, 1999. Textural features for grain identification. Agric. Eng. J., 8: 213-222.

Mallat, S.G., 1989. A theory for multiresolution signal decomposition: The wavelet representation. IEEE Trans. Pattern Anal. Mach. Intell., 11: 674-693.

Mojsilovic, A., M.V. Popovic and D.M. Rackov, 2000. On the selection of an optimal wavelet basis for texture characterization. IEEE. Trans. Image Process., 9: 2043-2050.

Paliwal, J., N.S. Shashidhar and D.S. Jayas, 1999. Grain kernel identification using kernel signature. Trans. ASAE., 42: 1921-1924.

Paliwal, J., N.S. Visen and D.S. Jayas, 2001. Evaluation of neural network architectures for cereal grain classification using morphological features. J. Agric. Eng. Res., 79: 361-370.

Sarlashkar, A.N., M. Bodruzzaman and M.J. Malkani, 1998. Feature extraction using wavelet transform for neural network based image classification. Proceedings of the Thirtieth Southeastern Symposium on System Theory, March 10, 1998, IEEE, Nashville, Tennessee, USA., ISBN:0-7803-4547-9, pp: 412-416.

Szczypinski, P.M. and P. Zapotoczny, 2012. Computer vision algorithm for barley kernel identification, orientation estimation and surface structure assessment. Comput. Electr. Agric., 87: 32-38.

Tamura, H., S. Mori and T. Yamawaki, 1978. Textural features corresponding to visual perception. IEEE Trans. Syst. Man Cybernetics, 8: 460-473.

Walker, J.S., 1999. A Primer on Wavelets and their Scientific Applications. Chapman & Hall-CRC, Boca Raton, Florida, USA.,.

Wiwart, M., E. Suchowilska, W. Lajszner and L. Graban, 2012. Identification of hybrids of spelt and wheat and their parental forms using shape and color descriptors. Comput. Electr. Agric., 83: 68-76.

Zheng, C., D.W. Sun and L. Zheng, 2006. Classification of tenderness of large cooked beef joints using wavelet and Gabor textural features. Trans. ASABE., 49: 1447-1454.